



Effect of microwave heating on the mechanical properties and energy dissipation characteristics of hard rock

Jian-ming Yang^{1,2} · Jiang-tian Liu¹ · Hong-chen Guo² · Qing-wen Li² · Wei Wang¹

Received: 16 September 2021 / Accepted: 14 July 2022 / Published online: 16 August 2022
© The Author(s), under exclusive licence to Springer-Verlag GmbH Germany, part of Springer Nature 2022

Abstract

To study the effect of microwave on the weakening mechanism of hard rock, uniaxial compression tests were conducted on granite samples after microwave treatment, and an acoustic emission system was established to monitor the fracture evolution in such rock samples. The effects of microwave irradiation on the stress–strain curve, acoustic emission characteristics, and energy dissipation characteristics of granite were investigated in the experiment. The results show that: (1) With the continuous increase of microwave irradiation power and time, the compaction stage and crack development stage of the sample gradually increase, and the elastic stage gradually becomes shorter; the trend of post-peak stress drop becomes slower, changing from “cliff type” to multi-step type “. The failure of the sample indicates that they become less brittle and more ductile; (2) Microwave irradiation reduces the strength. The overall acoustic emission count rate is weak before the peak and increases rapidly near the peak. The count rate has also changed from sparse to dense, and with the increase in the irradiation power and time, the total acoustic emission count rate increases; (3) From the energy point of view, the weakening of granite by microwave irradiation will not only decrease the energy-storage limit of granite and increase the proportion of dissipated energy in the failure process, but also decrease the rate of release of elastic energy after the peak. Therefore, microwave irradiation will not only reduce the mechanical energy dissipated during damage, but also reduce the intensity of potential dynamic disasters.

Keywords Rock mechanics · Microwave heating · Uniaxial compression · Mechanical properties · Acoustic emission characteristics · Energy dissipation

Introduction

With the increasing depletion of global shallow gold resources, many gold enterprises have entered the stage of kilometre-level or even deeper mining, such as the Mponeng gold mine in South Africa, where the depth of the mine shaft reaches 4530 m, and its ore body is buried deeper than 7500 m. At present, the main rock-breaking methods for gold mining are blasting and mechanical methods, which account for more than 90% (Xi-bing et al. 2010). Compared with shallow mining, the mechanical response of rock mass in deep complex geological environment exhibits a high degree

of non-linearity, especially in a high ground stress environment, the disturbance response of raw rock to blasting is further amplified, and it is easy to induce dynamic disasters such as loosening, spalling, and throwing of adjacent rock mass; meanwhile, the high stress increases the uniaxial compressive strength (UCS), tensile strength (BTS), wear resistance (CAI) of the rock mass, etc. This makes mechanical cutting and crushing more difficult; not only is the efficiency of rock-breaking low, but tool wear is also more severe.

In recent years, with the rapid development of microwave technology, many scholars have introduced microwave technology into the field of mining engineering. The research on microwave-assisted rock breaking can be traced back to the 1970s, when Gushchin et al. (1979) and Protasov et al. (1984) designed a road heading machine that combined the advantages of microwave and mechanical rock breaking. Since then, with the improvement of the working performance of tunnelling machinery, research into microwave-assisted rock breaking technology has not been continued.

✉ Qing-wen Li
18701187727@163.com

¹ China National Gold Group Co., Ltd., Beijing 100011, China

² School of Civil and Resource Engineering, University of Science and Technology Beijing, Beijing 100083, China

Until the increase of major construction projects such as underground dark matter laboratory, national defence engineering construction, and space mining exploration, microwave-assisted rock breaking technology has gradually become a focus of much research today. Hassani 2011, 2012, 2016; Satish et al. (2006); Nekoovaght et al. (2014) investigated the changes in the mechanical properties of rock under microwave irradiation, and the feasibility of microwave-assisted mechanical rock breaking in space mining was explored based on experiments and numerical simulations.

Microwave rock breaking utilises the different microwave absorption capacities of various minerals within the rock mass to generate an internal temperature gradient. When the generated thermal stress exceeds the chemical bond-strength in the mineral crystal or the cementing force between the crystals, it causes the minerals to fracture along or through the crystal, resulting in microscopic and macroscopic cracks within the specimen (Li et al. 2017). In the last two decades, scholars have conducted much research into the weakening effect of microwave heating paths on rocks. It was found that with the increase of microwave irradiation power and time, the macroscopic and microscopic cracking of rock increased, and the uniaxial compressive strength (Lu 2019a, b), tensile strength (Hassani et al. 2016), and point load strength (Hassani et al. 2016) decreased. Moreover, at a certain applied irradiation power, with the increase of the microwave irradiation time, the decrease in rock strength tends to be slight (Qinhua et al. 2020). In addition, researchers also studied these effects from the perspectives of rock mineral types and content (Batchelor et al. 2015; Motlagh et al. 2009), particle size (Rizmanoski et al. 2011), water content (Peinsitt et al. 2010; Jun et al. 2020), etc.

In summary, most existing studies have assessed the influence of microwaves on the mechanical properties of the rock from the perspective of the stress–strain curve after microwave heating treatment, and few studies have reported on the damage evolution and its strain energy conversion mechanism in the process of rock failure. In the present research uniaxial compression tests on granite treated by microwave heating were conducted, and the internal damage of the rock samples was monitored in real-time by an acoustic emission system. In addition, the mechanism of microwave weakening of granite was revealed from the perspective of acoustic emission characteristics and energy dissipation law.

Test programme

Equipment

The microwave heating equipment used in this experiment is an RWLM6 microwave high-temperature heating



Fig. 1 RWLM6 microwave high-temperature heating furnace



Fig. 2 GAW-2000 electro-hydraulic triaxial testing machine

furnace, the output power of the equipment is continuously adjustable from 0.1 to 6.49 kW, and the microwave frequency is $2.45 \text{ GHz} \pm 25 \text{ MHz}$; its internal cavity measures $150 \text{ mm} \times 150 \text{ mm} \times 110 \text{ mm}$, equipped with a microwave detector and probe, which can accurately monitor the surface temperature of the material in real-time. The experimental uniaxial compression uses a Rising Sun GAW-2000 microcomputer controlled electro-hydraulic servo-controlled rigid pressure testing machine. The equipment used in the experiment is shown in Figs. 1 and 2.

Heating path and loading path

The sample microwave heating process is as follows:

Microwave heating path 1: microwave irradiation at 1 kW, irradiation times of 1, 3, and 5 min, and the test group numbers are A, B, and C;

Microwave heating path 2: microwave irradiation at 3 kW, irradiation times of 1, 3, and 5 min, and the test group numbers are D, E, and F.

After reaching the microwave heating target, we stopped the microwave high-temperature furnace irradiation for 5 min, removed the specimen, then allowed it to cool to room temperature in the laboratory.

The rock samples were heated by microwave and placed in a GAW-2000 electro-hydraulic triaxial testing machine for uniaxial loading under a compressive stress that was increased at 0.5 MPa/s until failure. During testing, the PCI-II acoustic emission system of the American Physical Acoustics Company was used to monitor the acoustic emission signal in the process of rock sample fracture in real-time. The preamplifier gain, and departure threshold values were set to 40 dB, and the adopted frequency was 0.5 MHz.

Sample preparation

To reduce the spread of the test results, specimens were made from the same homogeneous granite block. The average density of the rock at room temperature is 2.68 g/cm³, and the average P-wave velocity is 6.326 km/s. The specimens measured Φ 30 mm \times 60 mm, the parallelism of the upper and lower end faces was controlled to within ± 0.05 mm, and the deviation of the end-face perpendicular to the axis of the sample does not exceed 0.25°. A partially processed specimen is shown in Fig. 3.

The density and P-wave velocity of granite samples before and after microwave heating are listed in Table 1. After microwave irradiation, both the sample density and P-wave velocity decrease with the increase of microwave



Fig. 3 Granite samples

Table 1 Sample density and P-wave velocity before and after microwave irradiation

Microwave heating method	Pre-irradiation density kg m ⁻³	Post-irradiation density kg m ⁻³	P-wave velocity km s ⁻¹
1 kW 1 min	2667	2658	5.880
1 kW 3 min	2667	2642	5.648
1 kW 5 min	2672	2625	5.220
3 kW 1 min	2673	2642	5.654
3 kW 3 min	2664	2625	5.131
3 kW 5 min	2656	2630	4.855

irradiation power and time: at the same irradiation time, the decrease at high power (3 kW) is greater than that at the lower power of 1 kW.

Analysis of test results under uniaxial compression

Stress–strain curve

The uniaxial stress–strain curves of the granite specimens under different microwave irradiation paths are shown in Fig. 4: the uniaxial compressive stress–strain curves evolve in a similar manner for each specimen, all passing through an initial fracture compaction closure stage (I), linear elastic deformation (II), stable crack development (III), non-stable crack development (IV), and a post-peak stage (V). However, it is found by comparison that the mechanical behaviour of the specimens under different microwave irradiation regimes differs: (1) Under the same irradiation power, the compaction phase is prolonged by an increased microwave irradiation time, and the elastic modulus decreases (the elastic moduli under irradiation at 1 kW and 3 kW for between 1 and 5 min are 30,173, 35,372, 34,298, and 34,766, 34,396, and 30,397, respectively). The minerals or inter-mineral cement in the specimen are damaged more severely with prolonged irradiation; (2) Under the same microwave irradiation time, the high-power specimen after the post-peak stress declines more slowly, showing that the damage caused by high-power irradiation to the interior of the rock sample is greater. As a result, the granite becomes less brittle and more ductile.

Determination of feature points

In the whole process of rock deformation and failure, scholars defined the key thresholds at the onset of each stage as the crack closure stress σ_{cc} , crack initiation stress σ_{ci} , damage stress σ_{cd} , and peak stress σ_{cf} (Martin and Chandler 1994; Hoek and Bieniawski 1965). The crack closure stress σ_{cc} is

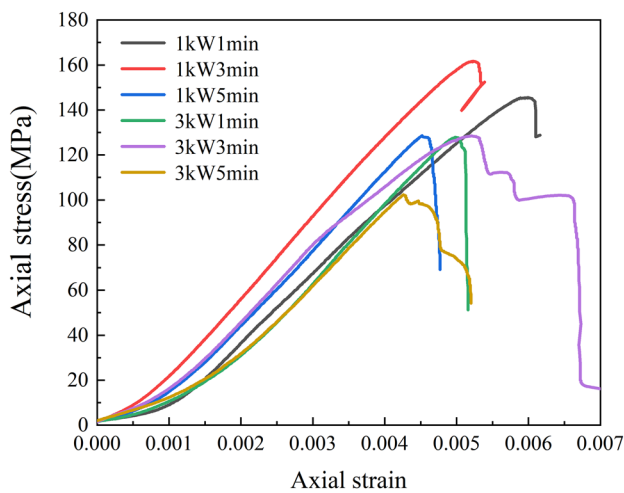


Fig. 4 Stress–strain curves of specimens under uniaxial compression

the stress corresponding to the maximum degree of closure of the internal pre-existing fracture in compression closure under load; the crack initiation stress σ_{ci} is the emergence of new cracks in the interior and the initiation point of rock failure; the damage stress σ_{cd} is triggered by the rapid development and coalescence of internal cracks, and marks the onset of the expansion of the rock; the peak stress σ_{cf} represents the ultimate bearing capacity of the rock under the current stress state.

The crack closure stress σ_{cc} and peak stress σ_{cf} are usually determined directly from the stress–strain curve, while the crack initiation stress σ_{ci} and damage stress σ_{cd} were calculated using the volumetric strain method (Brace et al. 1966), the transverse strain method (Lajtai 1974), and the acoustic emission characteristic point method (Eberhardt et al. 1998), numerical simulation (Huang and Li 2017). With the development of acoustic emission technology, subjective judgment is largely avoided, so the acoustic emission method is used here.

Diederichs et al. (2014) combined the change of stress-impact rate-cumulative impact rate-time curve and proposed the use of a linear auxiliary line to determine σ_{cd} . Figures 5 and 6 correspond to the evolution of acoustic emission count rate of heating paths 1 and 2. A typical 1 kW 3 min specimen was taken as an example (Fig. 5b): the original internal fissures of the specimen were gradually compressed and closed at the early stage of loading, accompanied by certain acoustic emission events and peaked at the end of the compaction stage (corresponding to $\sigma_{cc} = 26.076$ MPa); the acoustic emission count decreases after entering the elastic stage, the cumulative acoustic emission count rate rises linearly and slowly, and the acoustic emission count rate increases significantly at the end, indicating that the internal fissures of the specimen start to crack, and then the specimen enters the stable crack-development stage; the acoustic emission

count rate continues to increase therein, and the cumulative acoustic emission count rate increases in a non-linear manner; after entering the unstable crack-development stage, the acoustic emission count rate increases abruptly, and the cumulative acoustic emission count rate curve increases rapidly, indicating the rapid expansion and penetration of the internal cracks in the specimen.

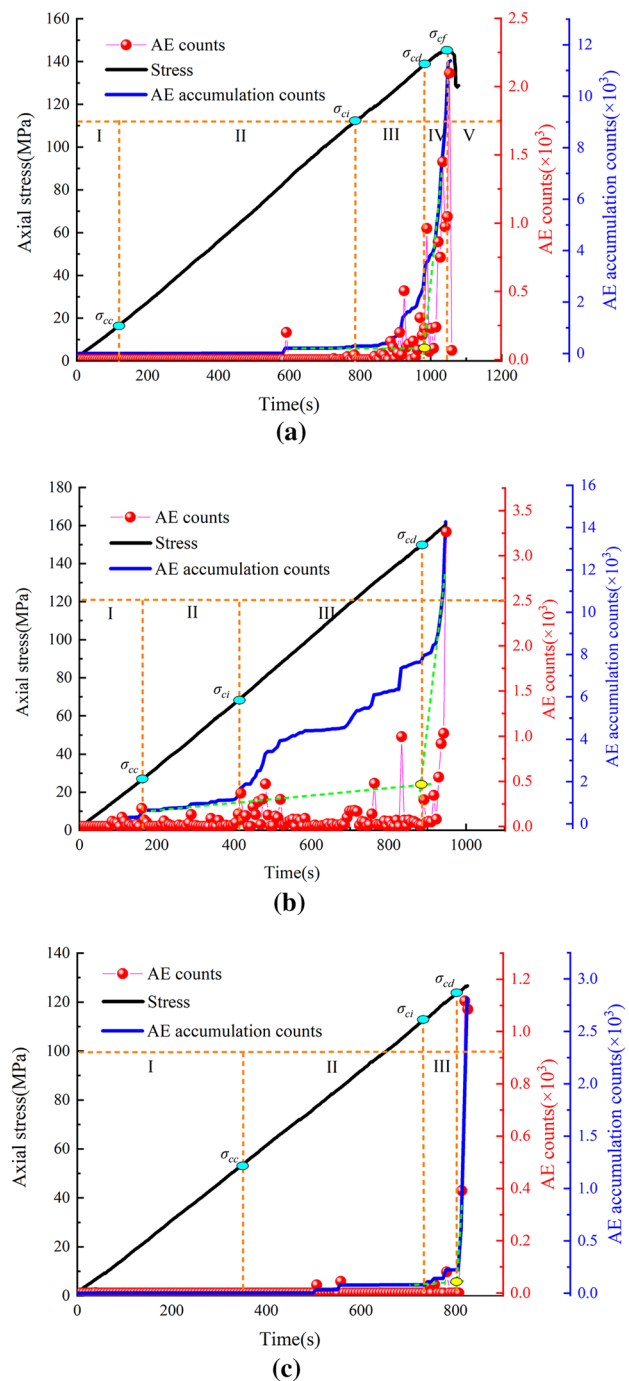


Fig. 5 Change of acoustic emission count rate under heating path 1. **a** 1 kW 1 min 0 MPa, **b** 1 kW 3 min 0 MPa, **c** 1 kW 5 min 0 MPa

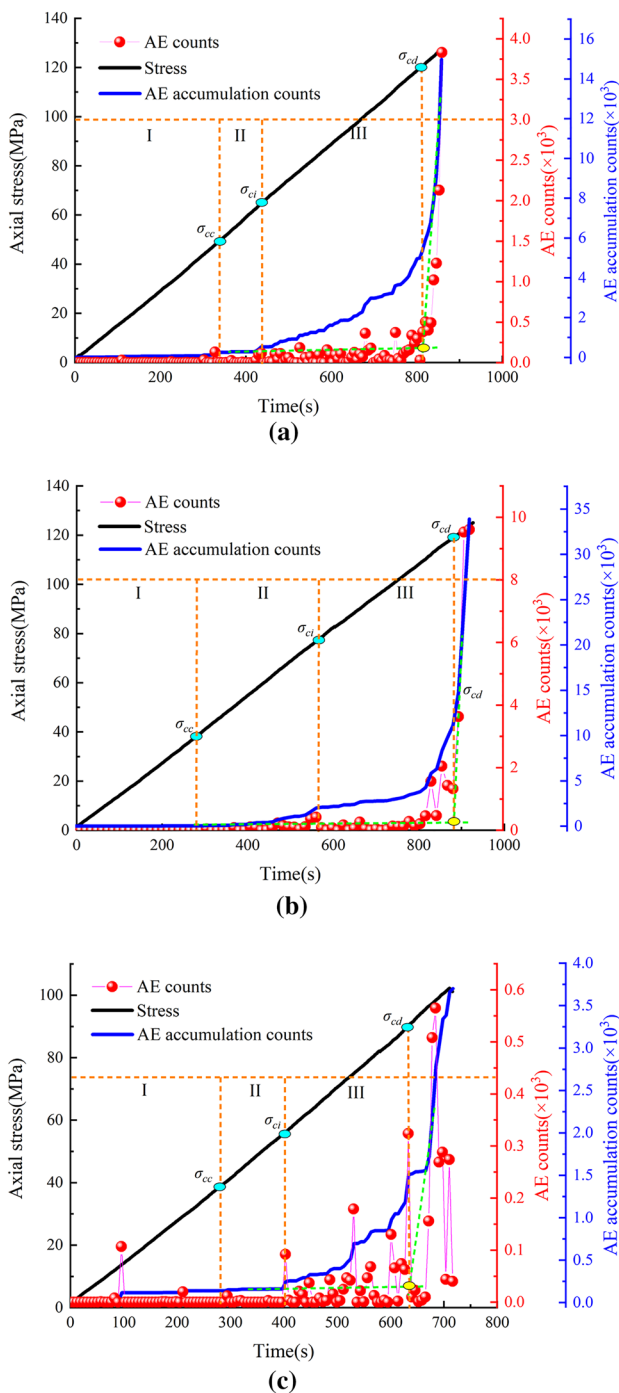


Fig. 6 Change of acoustic emission count rate under heating path 2. **a** 3 kW 1 min 0 MPa, **b** 3 kW 3 min 0 MPa, **c** 3 kW 5 min 0 MPa

Strength at the feature points

Under different microwave heating paths, the characteristic point stress during the failure process of the specimen is shown in Fig. 7: the crack closure stress σ_{cc} of the specimen tends to increase with increasing microwave time under the same power, and the stresses σ_{ci} , σ_{cd} , and σ_{cf} continue to

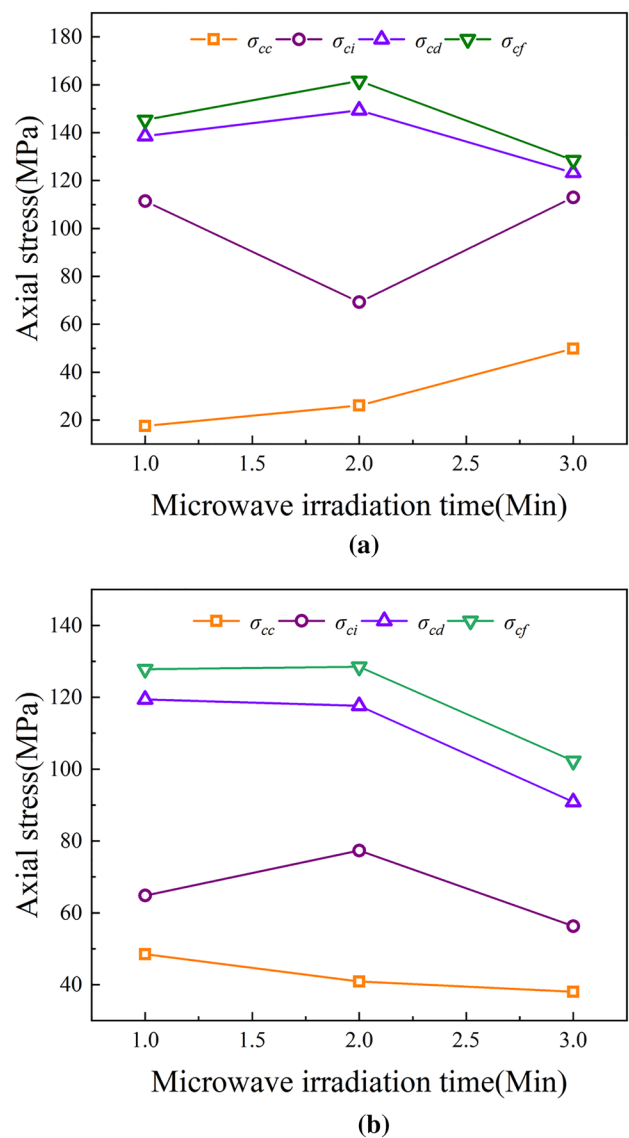
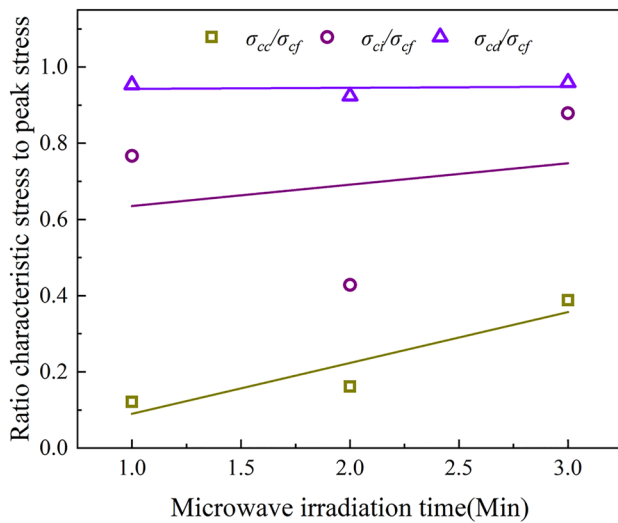


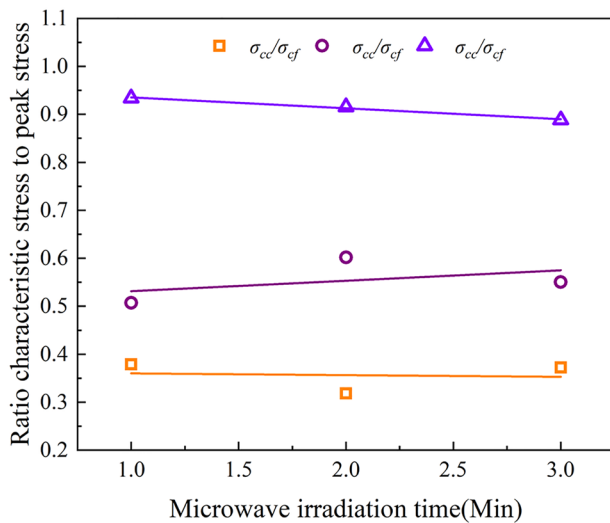
Fig. 7 Stress at characteristic points of specimens under uniaxial compression test. **a** Heating path 1, **b** Heating path 2

decrease. Under the same microwave irradiation time, σ_{cc} is higher under the action of high power (3 kW) than low power (1 kW), while the crack initiation stress σ_{ci} , damage stress σ_{cd} , and peak stress σ_{cf} are higher under low power rather than high power. This reflects the fact that the cracking point, damage point, and strength of granite decrease with rising microwave irradiation time and power, that is, the strength and hardness of granite are both decreased.

Considering the differences among the rock samples themselves, σ_{cc} , σ_{ci} , σ_{cd} , and σ_{cf} of each specimen were compared. As shown in Fig. 8, the rock crack closure stress σ_{cc} increases linearly with the increase of microwave irradiation time. The proportion of the compaction stage in the whole stress–strain curve increases, that is, the more severe the internal damage



(a)



(b)

Fig. 8 Ratio of characteristic point stress to peak stress. **a** Heating path 1, **b** Heating path 2

of the specimen, the more developed the cracks. In addition, under low-power irradiation, the values of σ_{cc} , σ_{ci} , σ_{cd} , and peak strength σ_{cf} of the rock are respectively $0.22\sigma_{cf}$, $0.69\sigma_{cf}$, and $0.95\sigma_{cf}$; under high-power irradiation, and $0.35\sigma_{cf}$, $0.55\sigma_{cf}$ and $0.91\sigma_{cf}$ under low-power irradiation (1 kW). This implies that the influence of microwave irradiation power on the mechanical properties of the specimen is larger than the irradiation time. At the same time, this relationship can be adopted to predict the crack initiation stress and damage stress.

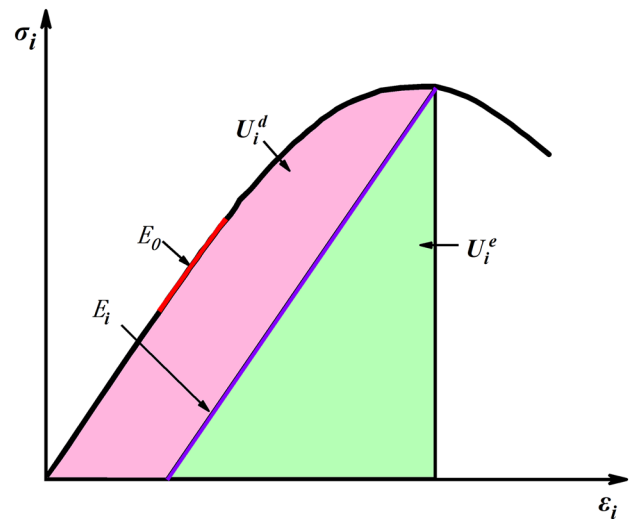


Fig. 9 Energy calculation diagram: loading to σ'

Energy evolution under uniaxial compression

Energy calculation

The laws of thermodynamics show that the deformation and destruction of materials is the intrinsic essence of the internal energy conversion process, and the destruction of rocks can be better analysed from the perspective of energy. Failure (in rock) is a progressive damage and rupture process. The energy is mainly present as elastic energy, plastic energy, thermal energy, radiation energy, kinetic energy, etc. (Xie et al. 2005). Limited by the existing monitoring technology, it is difficult to realise real-time monitoring of various forms of energy. Considering the proportion of various energy in the process of rock failure, we focus here on the total mechanical input energy, elastic deformation energy, and dissipation of energy (via plasticity and friction).

Assuming the deformation and failure of the rock under compression is a closed system, all mechanical work done by the external force is transformed and absorbed: the first law of thermodynamics gives:

$$U^0 = U^e + U^d \tag{1}$$

where U^0 is the work done by the loading test machine on the rock sample, U^e denotes the elastic energy and strain energy accumulated in the rock specimen, U^d is the energy dissipated by the deformation of the rock, which is mainly used for fracture initiation, expansion, and mineral particle deformation.

Figure 9 shows the stress–strain curve of an element in a rock mass: E^0 is the modulus of elasticity in the elastic stage, E^i is the unloading modulus of elasticity, U_i^e represents the

internal releasable deformation energy, and U_i^d represents the energy dissipated under deformation.

The total input work, elastic deformation energy, and dissipation of energy under uniaxial compression are given by:

$$U^0 = \int \sigma_1 d\varepsilon_1 = \sum_{i=1}^n \frac{1}{2} (\sigma_{i+1} + \sigma_i) (\varepsilon_{i+1} + \varepsilon_i) \quad (2)$$

$$U^e = \frac{\sigma_1^2}{2E_0} \quad (3)$$

where σ_i is the stress, and ε_i is the strain. It is worth mentioning that the elastic modulus is taken as the elastic modulus E_0 when calculating the energy in the present research.

Microwave effects on energy evolution

According to formulae (1) to (3), the energy evolution curve during the deformation process of the rock sample under different microwave irradiations is as shown in Figs. 10 and 11: under different microwave heating paths, the energy evolution during uniaxial compression deformation is similar. Before the peak, it shows energy accumulation and dissipation: post-peak, it shows energy release.

The main characteristics of energy evolution in each stage of rock compression deformation are: the crack closure and compaction stage (I): part of the work done by the testing machine on the rock sample is converted into elastic deformation energy and stored inside the rock sample. This part of elastic energy accounts for more than 53.6% of the total energy. The other part is dissipated, and contributes to closure of the original micro-cracks and the deformation of mineral particles.

Linear elastic deformation stage (II): the elastic energy change curve is close to the mechanical total input energy curve, and the dissipated energy curve is approximately parallel to the strain. At this stage, when the irradiation power is 1 kW, the elastic deformation energy accounts for 94.8% to 96.6% of the total energy. When the irradiation power is 3 kW, the elastic deformation energy accounts for 80.6% to 92.6% thereof.

Stable crack-development stage (III) and unsteady crack-development stage (IV): with the development and expansion of internal cracks in the rock sample, the amount of energy dissipated tends to increase and the rate of change thereof increases. At an irradiation power of 1 kW and 3 kW at this stage, the elastic energy accounted for 86% to 94.8% and 89.2% to 70.9% of the total mechanical input energy, respectively.

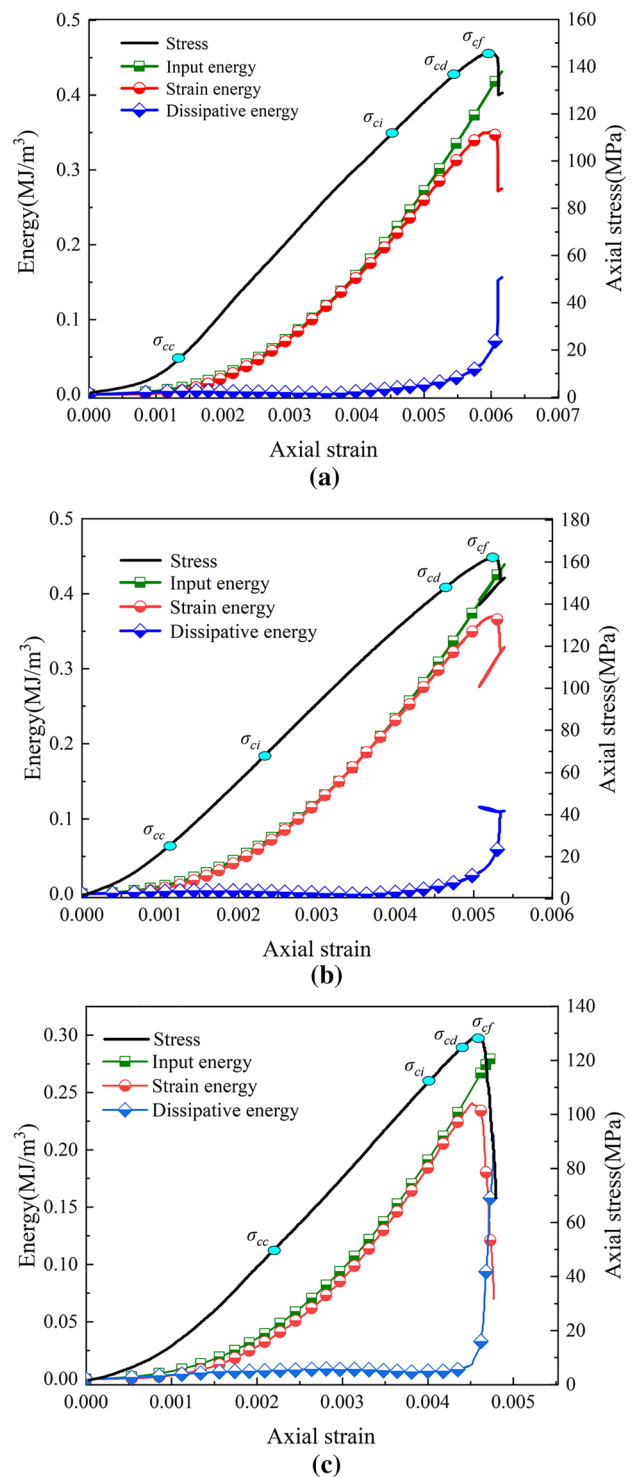


Fig. 10 Stress–strain–energy relationship: specimen irradiated at 1 kW. **a** 1 kW 1 min test piece, **b** 1 kW 3 min test piece, **c** 1 kW 5 min test piece

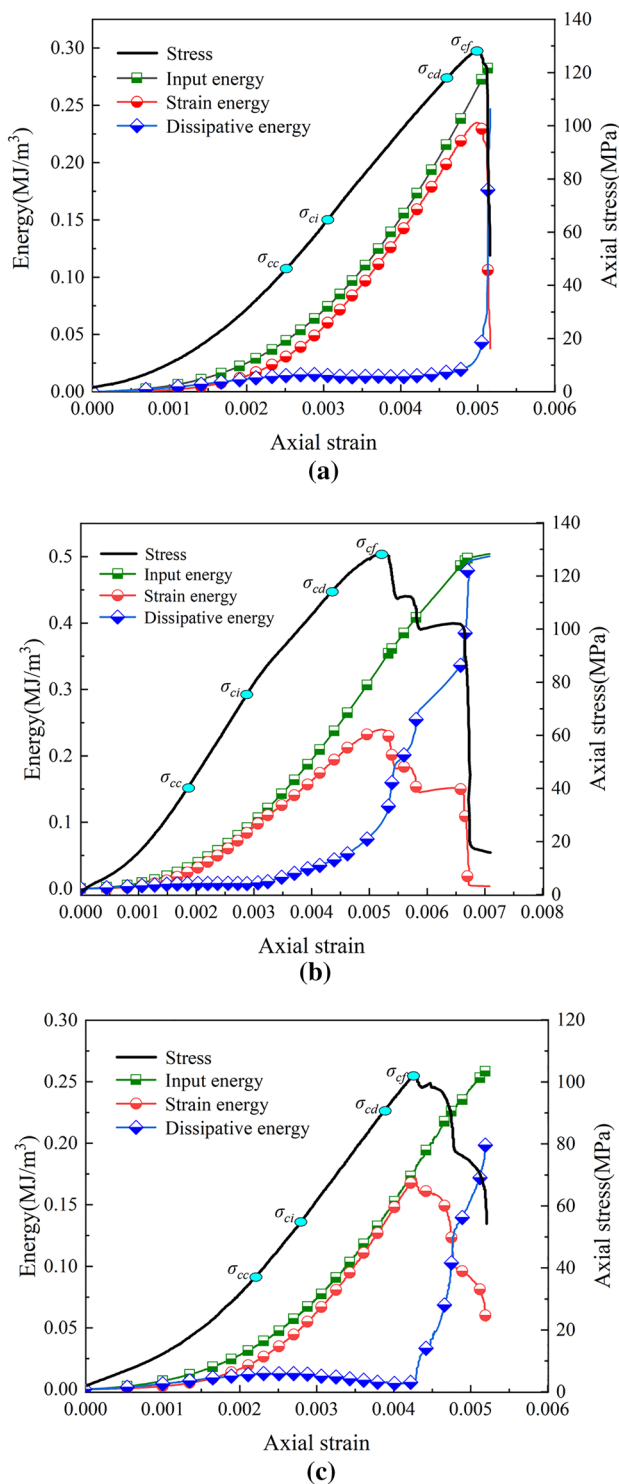


Fig. 11 Stress–strain–energy relationship: specimen irradiated at 3 kW. **a** 3 kW 1 min test piece, **b** 3 kW 3 min test piece, **c** 3 kW 5 min test piece

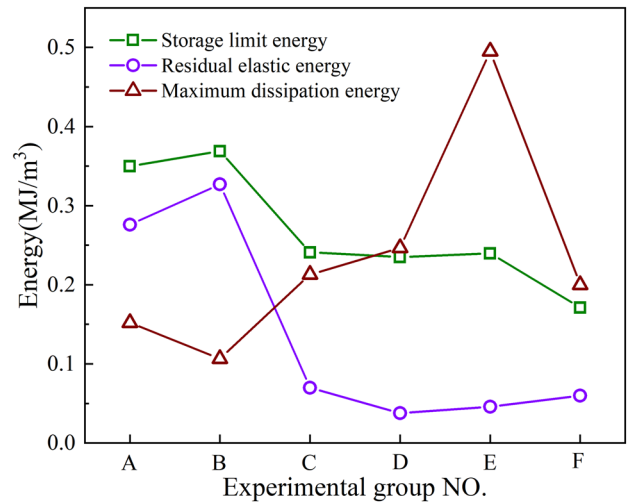


Fig. 12 Energy changes at special points in each rock specimen

Post-peak phase (V): the elastic energy stored inside the rock sample is released instantly, the elastic energy increases rapidly, and that dissipated increases sharply. At this stage, most of the work done by the testing machine is dissipated. The internal fissures of the rock penetrated rapidly, and significant macroscopic cracks appeared.

The energy storage limit, residual elastic density, and maximum energy dissipation in each specimen were extracted to further quantify the influence of microwave irradiation on rock samples (Fig. 12).

At 1 kW and 3 kW, the energy storage limits are 0.35, 0.37, 0.24, 0.25, 0.24, and 0.17 with the increasing irradiation times, respectively. The evolution of residual elastic energy is akin to the deformation of stored elastic energy, and both decrease with the increase of irradiation power and time, while the maximum energy dissipation shows the opposite trend. Therefore, in engineering practice, by increasing the microwave irradiation power and irradiation time, the energy storage limit and residual elastic energy of granite can be reduced. This will transfer the accumulated elastic energy to greater depth within the rock mass, reducing the threat of potential dynamic disasters.

Microwave effects on the energy dissipation ratio

Rock deformation and failure as an asymptotic damage process can usually be reflected by energy dissipation. To reduce the influence of the discreteness of the rock sample, the ratio of the dissipated energy of the specimen to the total input energy is defined as the energy dissipation ratio (Fig. 13). It can be seen from this that the evolution of the capacity dissipation ratio of each specimen is similar, and it generally shows a trend of “rapid rise-rapid decline-slow

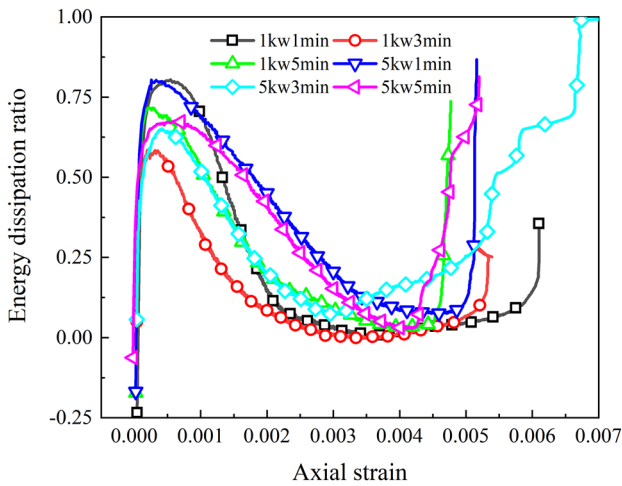


Fig. 13 Typical stress–strain–energy relationship

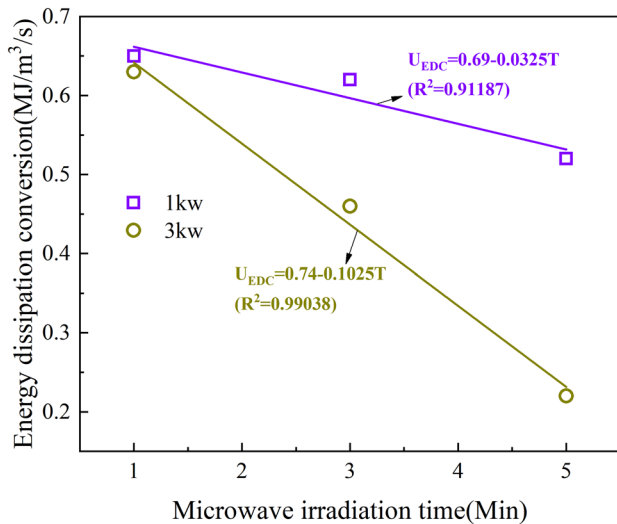


Fig. 14 Relationship between energy dissipation conversion and microwave irradiation time

decline-steep rise” as the strain increases, however, there are certain differences in the influence of microwave irradiation. Comparing rock samples, with the increase of microwave irradiation power and time in the pre-peak stage, the proportion of energy dissipated is found to increase. In the post-peak phase, the energy dissipation ratio rises at a different rate; for example, the 5 kW 3 min and 5 kW 5 min specimens rise in multiple steps after the peak stress is reached.

Microwave effects on the energy dissipation conversion rate

After the rock reaches its peak strength, the internal fissures develop and penetrate rapidly. The energy release rate after the peak is closely related to the conversion of the dissipated

energy at the peak stress. Dividing the increment of dissipated energy at the peak point by the corresponding time increment gives the conversion rate of dissipated energy at the peak point. According to data statistics, the relationship between the conversion rate of the energy dissipated in the specimen and the irradiation time is shown in Fig. 14.

It can be seen from the figure that under the same microwave irradiation time, the conversion rate of high-power energy dissipation energy is lower than that at low-power: as the irradiation time increases, the energy dissipation conversion rate under the action of high power decreases 3.15 times more than that at low power. This reflects the fact that with the increase of microwave irradiation power and time, the lower the conversion rate of dissipated energy at the peak stress on the granite specimens, the slower the rate of energy release after the peak. That is, microwave irradiation reduces the brittleness of the rock, and renders it more ductile, therefore, in the excavation of hard rock, the weakening of the rock mass by microwave irradiation can reduce the risk of dynamic disasters.

Conclusion

With the increase of microwave irradiation power and time, the longer the compaction stage and the mechanical development stage of the stress–strain curve, the slower the post-peak stress drop. The behaviour of granite changes from brittle to ductile at failure.

Under different microwave irradiation paths, the greater the initial damage to the sample, the more developed the internal fissures during the failure process, the stronger the acoustic emission count rate near the peak stress point, the lower the threshold of the intensity feature point, and the earlier the onset thereof.

After microwave irradiation, the energy storage limit and residual elastic energy density of granite are negatively correlated with irradiation power and time, and the maximum dissipated energy density is positively correlated therewith: under the same irradiation power, the peak energy dissipation conversion rate at 3 kW is 3.15 times that at 1 kW at a given time.

Author contributions All authors contributed to the study conception and design. Material preparation, data collection and analysis were performed by YANG Jian-ming, LIU Jiang-tian, GUO Hong-chen, LI Qing-wen, WANG Wei. YANG Jian-ming wrote the first draft of the manuscript. All authors commented on previous versions of the manuscript. All authors read and approved the final manuscript.

Funding This research is supported by the National Natural Science Foundation of China and Shandong Province Joint Program,

Fundamental Research Funds for the Central Universities, and Interdisciplinary Research Project for Young Teachers of USTB (Grants U1806209 NSFC, FRF-TP-19-021A3, and FRA-IDRY-19-002).

Availability of data and materials The datasets used or analysed during the current study are available from the corresponding author on reasonable request.

Declarations

Conflict of interest We declare that we do not have any commercial or associative interest that represents a conflict of interest in connection with the work submitted.

References

- Batchelor AR, Jones DA, Plint S, Kingman SW (2015) Deriving the ideal ore texture for microwave treatment of metalliferous ores. *Miner Eng* 84:116–129
- Brace WF, Paulding BW, Scholz C (1966) Dilatancy in the fracture of crystalline rocks. *J Geophys Res.* <https://doi.org/10.1029/JZ071i016p03939>
- Dan H, Xiao-qing L (2017) Numerical simulation research on characteristic strength of marble based on development of microcrack. *Rock Soil Mech* 38(01):253–262
- Diederichs MS, Kaiser PK, Eberhardt E (2014) Damage initiation and propagation in hard rock during tunnelling and the influence of near-face stress rotation. *Int J Rock Mech Min Sci* 41(5):785–812
- Eberhardt E, Stead D, Stimpson B et al (1998) Identifying crack initiation and propagation thresholds in brittle rock. *Can Geotech J* 35(2):222–233
- Gushchin VV, Kuznetsov VV, Chernikov VA et al (1979) Driving horizontal workings by means of an entry drifting machine with electrothermomechanical cutting. *Soviet Mining* 15(2):133–137
- Hassani F, Nekoovaght P (2012) The use of microwave to contribute to breakage of rocks[C]/2nd South American Symposium on Rock Excavations. San José, Costa Rica: [s. n.].
- Hassani F, Nekoovaght PM, Gharib N (2016) The influence of microwave irradiation on rocks for microwave- assisted underground excavation. *J Rock Mech Geotech Eng* 8(1):1–15
- Hassani F, Nekoovaght PM, Radziszewski P, et al. (2011) Microwave assisted mechanical rock breaking[C] Proceedings of the 12th ISRM International Congress on Rock Mechanics. Beijing: International Society for Rock Mechanics, 2075–2080
- Heping X, Yang J, Liyun L (2005) Criteria for strength and structural failure of rocks based on energy dissipation and energy release principles. *Chin J Rock Mech Eng* 17:3003–3010
- Hoek E, Bieniawski ZT (1965) Brittle fracture propagation in rock under compression. *Int J Fract* 1(3):137–155
- Jun D, Feifei Y, Shuilin X et al (2020) Experimental study on damage mechanism of basalt by microwave irradiation. *Sci Technol Eng* 20(7):2614–2618
- Lajtai EZ (1974) Brittle fracture in compression. *Int J FractMech* 10(4):525–536
- Lu GM, Feng XT, Li YH et al (2019a) Experimental investigation on the effects of microwave treatment on basalt heating, mechanical strength, and fragmentation. *Rock Mech Rock Eng* 52:2535–2549
- Lu GM, Feng XT, Li YH et al (2019b) The microwave- induced fracturing of hard rock. *Rock Mech Rock Eng* 52:3017–3032
- Martin CD, Chandler NA (1994) The progressive fracture of Lac du Bonnet granite. *Int J Rock Mech Min Sci Geomech Abstr* 31(6):643–659
- Motlagh PN (2009) An investigation on the influence of microwave energy on basic mechanical properties of hard rocks [D]. Concordia University, Montreal
- Nekoovaght P, Hassani F (2014) The influence of microwave radiation on hard rocks as in microwave assisted rock breakage applications[M]. *Rock engineering and rock mechanics structures in and on rock masses*. CRC Press, UK, pp 195–198
- Peinsitt T, Kuchar F, Hartlieb P et al (2010) Microwave heating of dry and water saturated basalt, granite and sandstone. *Int J Min Miner Eng* 2(1):18–29
- Protasov YI, Kuznetsov VV, Merzon AG et al (1984) A study of electrothermomechanical destruction of hard rocks with a rotary heading machine. *Soviet Min* 20(6):462–467
- Qinhua Z, Xiaobao Z, Yanlong Z et al (2020) A review on mineral heating characteristics and rock weakening effect under microwave irradiation. *Geol J China Univ* 26(3):350–360
- Rizmanoski V (2011) The effect of microwave pretreatment on impact breakage of copper ore. *Miner Eng* 24(14):1609–1618
- Satish H, Ouellet J, Raghavan V et al (2006) Investigating microwave assisted rock breakage for possible space mining applications. *Min Technol* 115(1):34–40
- Xi-bing L, Zi-long Z, Wei-hua W (2010) The status and prospect of development in rock fragmentation engineering [C] report on the development of rock mechanics and rock engineering discipline in 2009–2010. Beijing 2010:142–149 (in Chinese)
- Yuan-hui L, Gao-ming L, Xia-ting F et al (2017) The influence of heating path on the effect of hard rock fragmentation using microwave assisted method. *Chin J Rock Mech Eng* 36(6):1460–1468

Publisher's Note Springer Nature remains neutral with regard to jurisdictional claims in published maps and institutional affiliations.

Springer Nature or its licensor holds exclusive rights to this article under a publishing agreement with the author(s) or other rightsholder(s); author self-archiving of the accepted manuscript version of this article is solely governed by the terms of such publishing agreement and applicable law.